A

TS	KO system	In oncogenic *Kras*-driven models	In oncogenic *EGFR*-driven models
Pool			
Apc	CRISPR	Sánchez-Rivera *et al.*, 2014; Rogers *et al.*, 2017; Rogers *et al.*, 2018	
Arid1a	CRISPR	Walter *et al.*, 2017; Rogers *et al.*, 2017; Rogers *et al.*, 2018	
Atm	Null alleles; Cre/loxP; CRISPR	Efeyan *et al.*, 2009; Schmitt et al., 2017; Rogers *et al.*, 2017; Rogers *et al.*, 2018	
Cdkn2a	Null alleles; Cre/loxP; CRISPR	Fisher et al., 2001; Schuster *et al.*, 2014; Rogers *et al.*, 2017; Rogers *et al.*, 2018	
Keap1	CRISPR	Romero *et al.*, 2017; Rogers *et al.*, 2017; Rogers *et al.*, 2018	
Rb1	Cre/loxP; CRISPR	Ho *et al.*, 2009; Rogers *et al.*, 2017; Rogers *et al.*, 2018; Walter *et al.*, 2019	No published data
Rbm10	CRISPR	Rogers *et al.*, 2017; Rogers *et al.*, 2018	
Setd2	CRISPR	Walter *et al.*, 2017; Rogers *et al.*, 2017; Rogers *et al.*, 2018	
Smad4	CRISPR	Rogers *et al.*, 2017; Rogers *et al.*, 2018	
Lkb1	Cre/loxP; CRISPR	Ji *et al.*, 2007; Rogers *et al.*, 2017; Rogers *et al.*, 2018	
p53	Cre/loxP; CRISPR	Jackson *et al.*, 2005; Rogers *et al.*, 2017; Rogers *et al.*, 2018	
Others			
Cdkn2a/b	Cre/loxP	Schuster *et al.*, 2014	
Dnmt3a	Cre/loxP	Goa *et al.*, 2011	
Kdm6a	Cre/loxP	Wu *et al.*, 2018	
Nf1	CRISPR	Wang *et al.*, 2019	No published data
Pten	Cre/loxP; CRISPR	Iwanaga *et al.*, 2008; Curry *et al.*, 2013; Sánchez-Rivera *et al.*, 2014	
Smarca4	CRISPR	Walter *et al.*, 2017	
Tsc1	Cre/loxP	Liang *et al.*, 2010	
Notch2	Cre/loxP	Baumgart *et al.*, 2014	
Mig6	Null alleles		Maity *et al.*, 2015

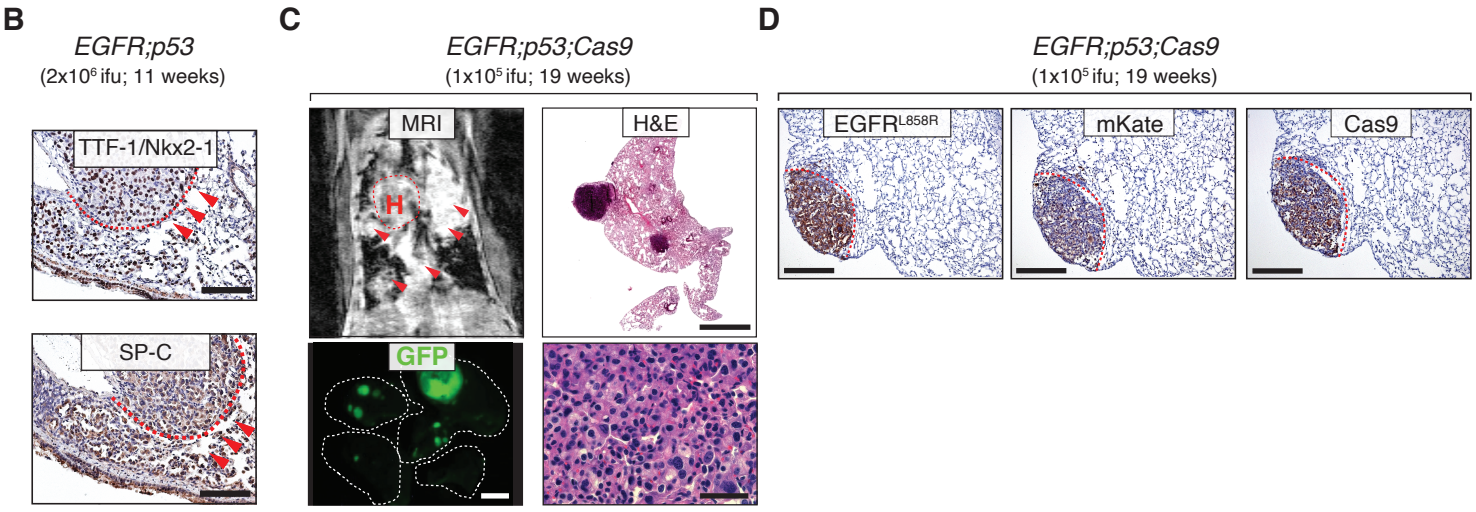

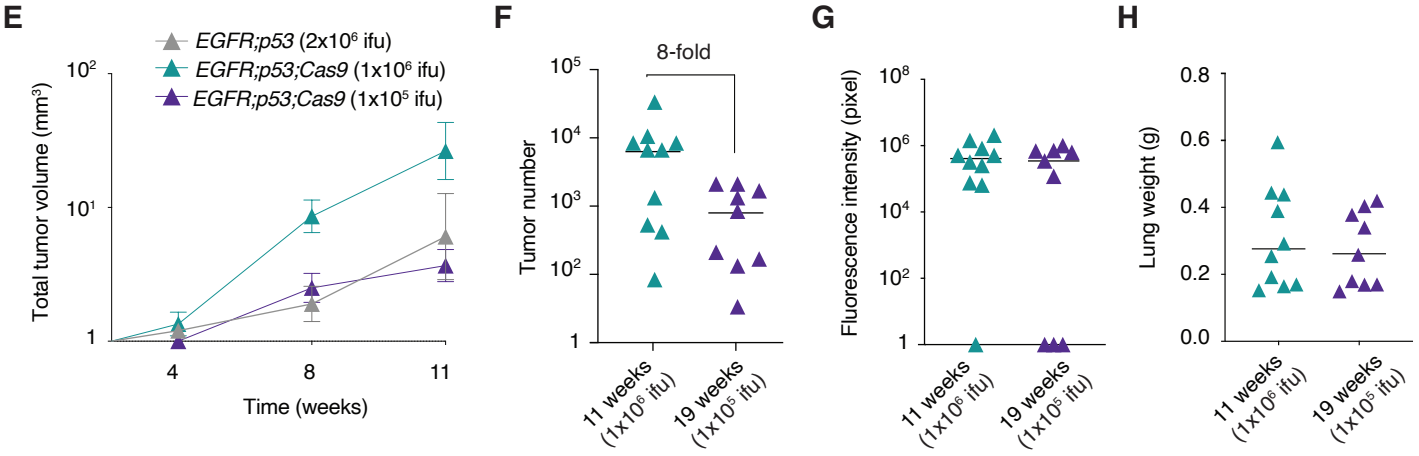

Supplementary Figure S1. Characteristics of lung tumors in *EGFR;p53* and *EGFR;p53;Cas9* mice.

A. Summary of the studies on tumor suppressor gene inactivation *in vivo*. Very few published data are currently available for the *EGFR*-driven lung cancer model.
B. Immunohistochemical staining showing a tumor positive for TTF-1/Nkx2-1 and SP-C in *EGFR;p53* mice. Red arrows indicate tumor areas. Scale bars = 100 μm.
C. MRI showing tumor development 19 weeks after tumor initiation in a representative *EGFR;p53;Cas9* mouse ($N = 9$) following delivery with $1x10^5$ ifu of Lenti-sg*TS*^{Pool}*/Cre* virus. H&E staining showing lung adenocarcinomas (right panels). Scale bars = 1.2 mm and 100 μm for the top and bottom panel, respectively. The dashed lines indicate the lungs. GFP image scale bar = 2.5 mm.
D. Immunohistochemical staining for EGFR^{L858R}, mKate and Cas9 after 19 weeks of tumor initiation in a representative *EGFR;p53;Cas9* mouse. The red lines indicate tumor areas. Scale bars = 200 μm.
E. Tumor growth curves in *EGFR;p53* and *EGFR;p53;Cas9* mice transduced with Lenti-sg*TS*^{Pool}*/Cre* virus quantified by measuring tumor volume by MRI at the indicated time points. Each triangle indicates the average of all tumor volumes from each group. Standard errors of the mean are shown.
F. Comparison of tumor number determined by Tuba-seq in *EGFR;p53;Cas9* mice transduced with Lenti-sg*TS*^{Pool}*/Cre* virus ($1x10^6$ versus $1x10^5$ ifu). Tumors initiated with a lower titer for 19 weeks are bigger and significantly fewer compared to tumors transduced with $1x10^6$ ifu of Lenti-sg*TS*^{Pool}*/Cre* virus. Each triangle represents a mouse. Horizontal lines show the median.
G. GFP quantification of tumor burden in *EGFR;p53;Cas9* mice after 11 or 19 weeks of tumor initiation. Horizontal lines show the median.
H. Tumor burden represented as the weight of tumor-bearing lungs in *EGFR;p53;Cas9* mice after 11 and 19 weeks of tumor initiation. Horizontal lines indicate the median.

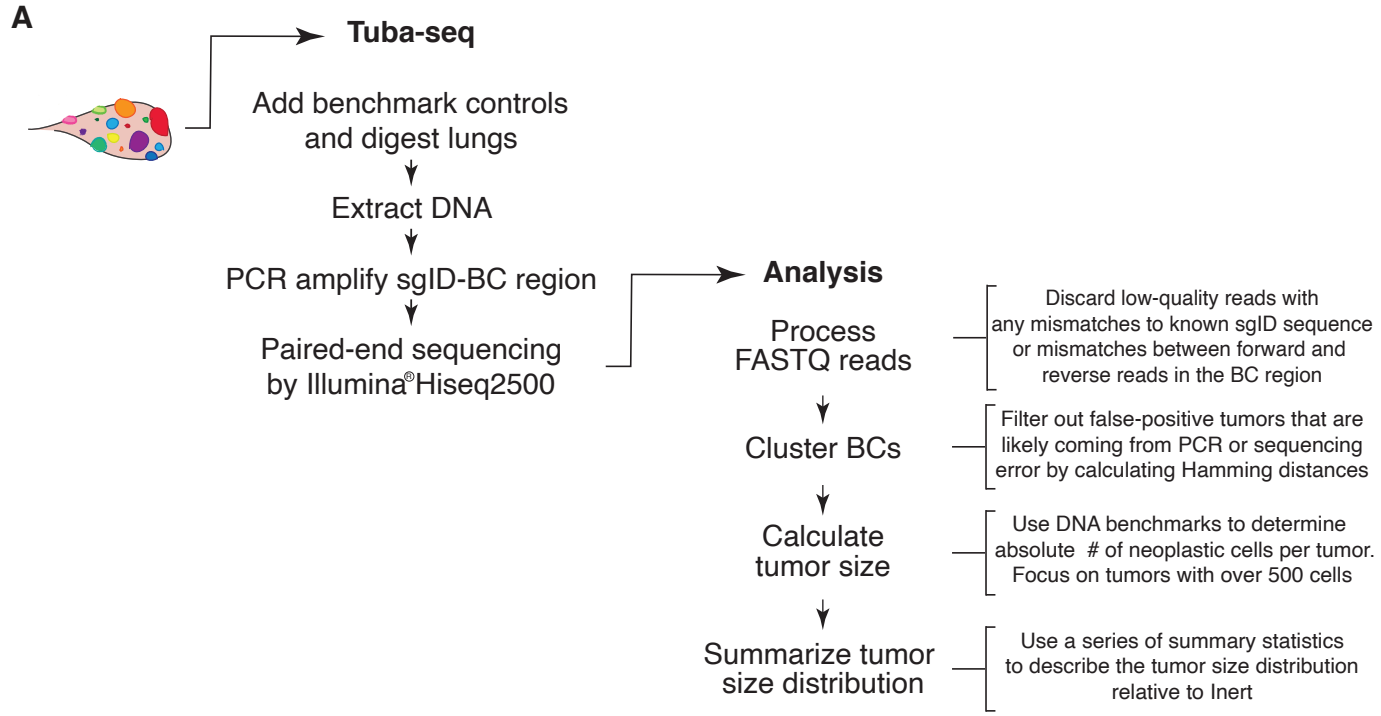

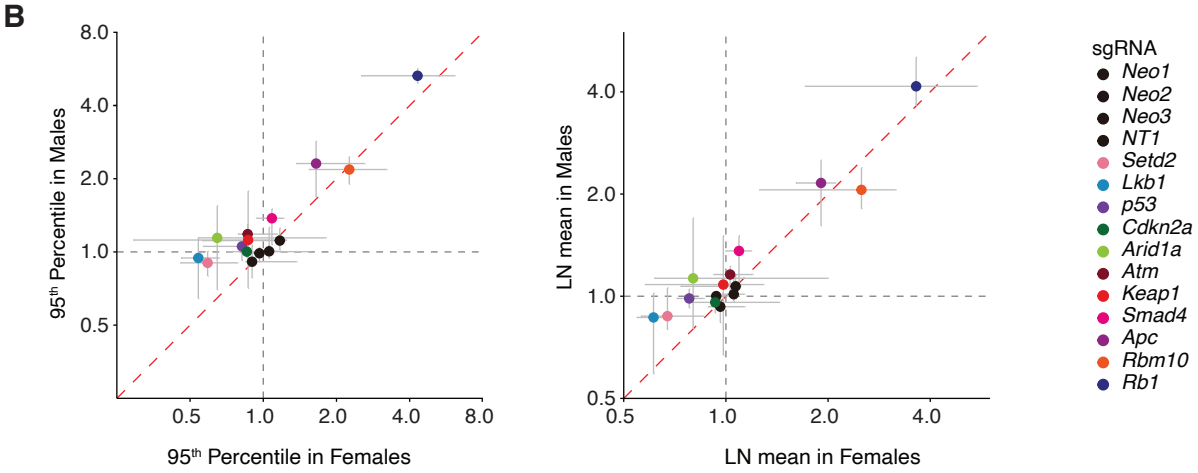

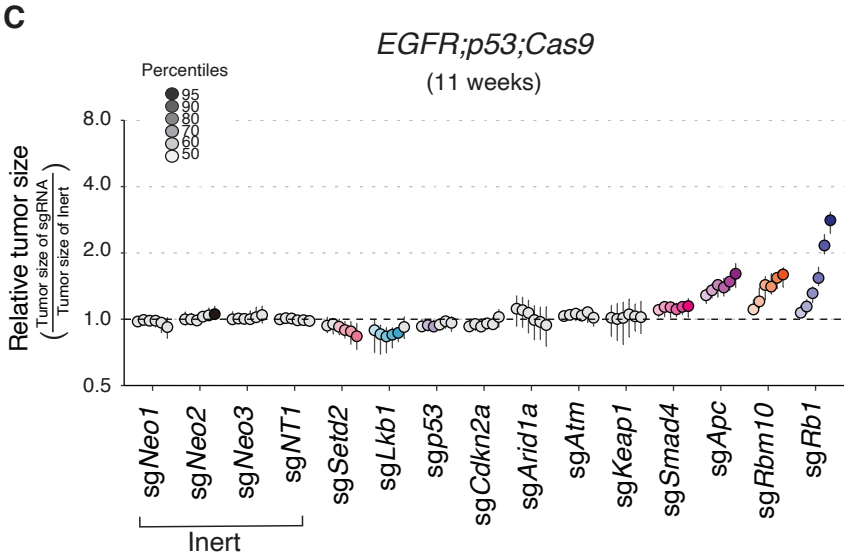

D

EGFR;p53;Cas9

	mean	*P*-value
sg*Rb1*	2.17	$<10^{-4}$
sg*Rbm10*	1.56	$<10^{-4}$
sg*Apc*	1.53	$<10^{-4}$
sg*Smad4*	1.15	0.02
sg*Keap1*	1.03	0.77
sg*Atm*	1.06	0.41
sg*Arid1a*	1.05	0.66
sg*Cdkn2a*	0.97	0.22
sg*p53*	0.97	0.25
sg*Lkb1*	0.90	$<10^{-4}$
sg*Setd2*	0.90	0.02
Inert: sg*Neo1*	0.97	0.15
Inert: sg*Neo2*	1.04	0.11
Inert: sg*Neo3*	1.01	0.59
Inert: sg*NT*	0.99	0.34

Supplementary Figure S2. Description of the Tuba-seq pipeline analysis and robustness of our model.

A. Tuba-Seq pipeline to quantify tumor sizes *in vivo*. Illumina® sequencing of the DNA barcode region of the integrated lentiviral vectors enables precise measurement of tumor size (see Supplementary Methods). First, reads with poor quality were discarded. Next, reads were piled-up into groups with unique barcodes. Read pileups were translated into absolute neoplastic cell number using the benchmark controls and by establishing a minimum cell number cutoff to call tumors (cutoff = 500 cells). Lastly, statistical analyses to describe the tumor size distribution were applied.

B. Effects of sex on the growth of *EGFR;p53;Cas9* tumors. Size distribution of *EGFR;p53;Cas9* tumors at the 95th percentile (left panel) 11 weeks after tumor initiation with Lenti-sg*TS^{Pool}/Cre* separately for males (N = 4) and females (N = 6) mice. Error bars showing the 95% confidence intervals after bootstrapping. LN mean (right panel) for tumors in *EGFR;p53;Cas9* mice 11 weeks after tumor initiation with Lenti-sg*TS^{Pool}/Cre* based on mouse sex. Each dot represents an sgRNA as indicated and the gray horizontal and vertical bars show the 95% confidence intervals.

C. Relative size distribution of *EGFR;p53;Cas9* tumors at different percentiles 11 weeks after tumor initiation, after simulating a 50% sgRNA efficiency reduction (N = 10). Error bars showing the 95% confidence intervals after bootstrapping. Percentiles that are significantly different from the tumors with inert sgRNAs are in color.

D. LN mean for tumors with each sgRNA in *EGFR;p53;Cas9* mice 11 weeks after tumor initiation after simulating a 50% sgRNA efficiency reduction (normalized to the tumors with inert sgRNAs). P-values are calculated from bootstrapping. P-values < 0.05 and their corresponding means are highlighted for sgRNAs that positively (red) and negatively (green) affect tumor growth when the effects are equal to or differ >10% compared to the size of tumors with inert sgRNAs.

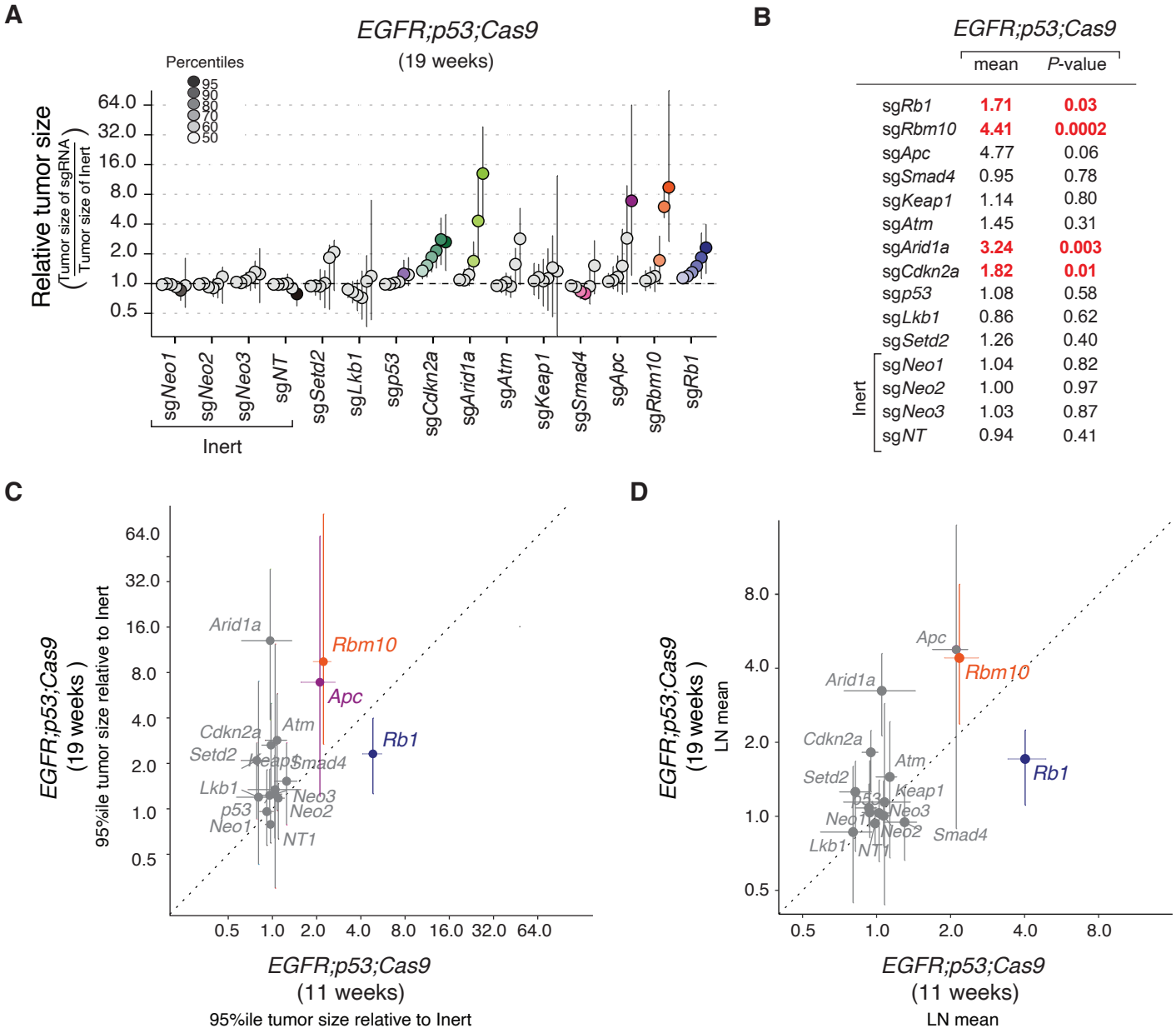

Supplementary Figure S3. Tuba-seq uncovers positive and negative effects of putative tumor suppressor gene inactivation on *EGFR*-driven lung tumor growth.

A. Relative size of tumors of each genotype in *EGFR;p53;Cas9* mice ($N = 9$) 19 weeks after tumor initiation with Lenti-sg*TS*^{Pool}*/Cre* virus. *P*-values are calculated from bootstrapping. Percentiles that are significantly different from the tumors with inert sgRNAs are in color. 95% confidence intervals are shown.

B. LN mean for tumors with each sgRNA in *EGFR;p53* and *EGFR;p53;Cas9* mice 19 weeks after tumor initiation (normalized to the tumors with inert sgRNAs). *P*-values are calculated from bootstrapping. *P*-values < 0.05 and their corresponding means are highlighted bold when the size effects are equal to or >10% compared to the size of tumors with inert sgRNAs.

C. Comparison of the relative effect of tumor suppressor gene inactivation in *EGFR;p53;Cas9* mice after 11 (X-axis) and 19 weeks (Y-axis) after tumor initiation. Relative tumor size for each sg*TS* compared to inert at the 95th percentile 11 and 19 weeks after tumor initiation with 1x10^6 and 1x10^5 ifu of Lenti-sg*TS*^{Pool}*/Cre* virus respectively (*EGFR;p53;Cas9* mice, 11 weeks $N = 10$; *EGFR;p53;Cas9* mice, 19 weeks $N = 9$). Error bars show the 95% confidence intervals. Genotypes that are significantly different from the inert tumors for both time-points are highlighted in color.

D. Relative LN mean comparison of tumor suppressor gene inactivation in *EGFR;p53;Cas9* after 11 and 19 weeks after tumor initiation. 95% confidence intervals are shown. Only genotypes that are significantly different from the inert for both time points, are highlighted in color.